Journal Pre-proof

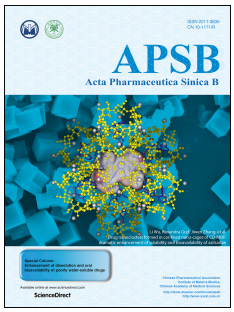

Notoginsenoside Ft1 acts as a *Tgr5* agonist but *Fxr* antagonist to alleviate high fat diet-induced obesity and insulin resistance in mice

Lili Ding, Qiaoling Yang, Eryun Zhang, Yangmeng Wang, Siming Sun, Yingbo Yang, Tong Tian, Zhengcai Ju, Linshan Jiang, Xunjiang Wang, Zhengtao Wang, Wendong Huang, Li Yang

PII: S2211-3835(21)00110-6

DOI: https://doi.org/10.1016/j.apsb.2021.03.038

Reference: APSB 1060

To appear in: *Acta Pharmaceutica Sinica B*

Received Date: 8 January 2021

Revised Date: 7 March 2021

Accepted Date: 10 March 2021

Please cite this article as: Ding L, Yang Q, Zhang E, Wang Y, Sun S, Yang Y, Tian T, Ju Z, Jiang L, Wang X, Wang Z, Huang W, Yang L, Notoginsenoside Ft1 acts as a *Tgr5* agonist but *Fxr* antagonist to alleviate high fat diet-induced obesity and insulin resistance in mice, *Acta Pharmaceutica Sinica B*, https://doi.org/10.1016/j.apsb.2021.03.038.

Graphical abstract

Notoginsenoside Ft1 activates *Tgr5*, but antagonizes *Fxr*, in ileum to enhance bile acid synthesis, thereby imparting metabolic improvement in high fat diet induced obese mice.

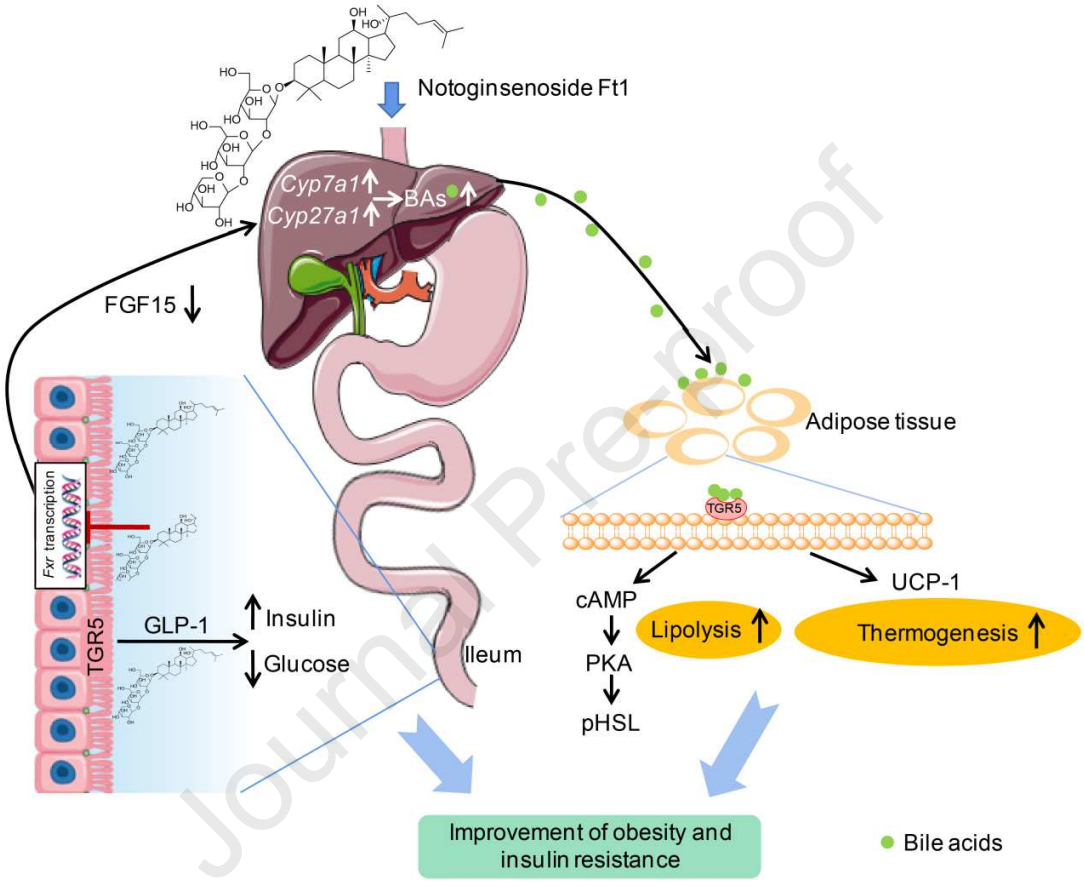

Original article

Notoginsenoside Ft1 acts as a *Tgr5* agonist but *Fxr* antagonist to alleviate high fat diet-induced obesity and insulin resistance in mice

Lili Ding[a,b], Qiaoling Yang[a,b,e], Eryun Zhang[a,b], Yangmeng Wang[b], Siming Sun[b], Yingbo Yang[a,f], Tong Tian[a,f], Zhengcai Ju[a], Linshan Jiang[a], Xunjiang Wang[a], Zhengtao Wang[a], Wendong Huang[b,c,*], Li Yang[a,d,*]

[a]*Shanghai Key Laboratory of Complex Prescriptions and MOE Key Laboratory for Standardization of Chinese Medicines, Institute of Chinese Materia Medica, Shanghai University of Traditional Chinese Medicine, Shanghai 201203, China*

[b]*Department of Diabetes Complications and Metabolism, Diabetes and Metabolism Research Institute, Beckman Research Institute, City of Hope National Medical Center, Duarte, CA 91010, USA*

[c]*Graduate School of Biological Science, City of Hope National Medical Center, Duarte, CA 91010, USA*

[d]*Institute of Interdisciplinary Integrative Medicine Research, Shanghai University of Traditional Chinese Medicine, Shanghai 201203, China*

[e]*Department of Pharmacy, Shanghai Children's Hospital, Shanghai Jiao Tong University, Shanghai 200040, China*

[f] *Current address: Jiangsu Kanion Pharmaceutical Co., Ltd., Lianyungang 222001, China*

Received 8 January 2021; received in revised form 7 March 2021; accepted 10 March 2021

[*]Corresponding authors. Tel.: +1 626 258 1203, fax: +1 626 256 8704 (Wendong Huang); Tel.: +86 21 51322506, fax: +86 21 51322519 (Li Yang).

E-mail addresses: whuang@coh.org (Wendong Huang), yangli7951@hotmail.com (Li Yang).

Running title: Notoginsenoside Ft1 acts as a *Tgr5* agonist but *Fxr* antagonist

Abstract Obesity and its associated complications are highly related to a current public health crisis around the world. A growing body of evidence has indicated that G-protein coupled bile acid (BA) receptor TGR5 (also known as Gpbar-1) is a potential drug target to treat obesity and associated metabolic disorders. We have identified notoginsenoside Ft1 (Ft1) from *Panax notoginseng* as an agonist of TGR5 *in vitro*. However, the pharmacological effects of Ft1 on diet-induced obese (DIO) mice and the underlying mechanisms are still elusive. Here we show that Ft1 (100 mg/100 diet) increased adipose lipolysis, promoted fat browning in inguinal adipose tissue and induced glucagon-like peptide-1 (GLP-1) secretion in the ileum of wild type but not *Tgr5*$^{-/-}$ obese mice. In addition, Ft1 elevated serum free and taurine-conjugated bile acids (BAs) by antagonizing *Fxr* transcriptional activities in the ileum to activate *Tgr5* in the adipose tissues. The metabolic benefits of Ft1 were abolished in *Cyp27a1*$^{-/-}$ mice which have much lower BA levels. These results identify Ft1 as a single compound with opposite activities on two

key BA receptors to alleviate high fat diet-induced obesity and insulin resistance in mice.

KEY WORDS Notoginsenoside Ft1; Obesity; Insulin resistance; Bile acids; TGR5; FXR; Glucagon-like peptide 1; Metabolic disorders

Abbreviations: ANOVA, analysis of variance; AUC, area under the curve; BAs, bile acids; BAT, brown adipose tissue; cAMP, adenosine 3′,5′ cyclic monophosphate; DIO, diet-induced obesity; eWAT, epididymal white adipose tissue; FGF, fibroblast growth factor; *Fxr*, nuclear farnesoid X receptor; GLP-1, glucagon-like peptide-1; *Tgr5*, membrane-bound G protein-coupled receptor; HFD, high fat diet; GTT, glucose tolerance test; ITT, insulin tolerance test; iWAT, inguinal white adipose tissue; KO, knockout; Ft1, notoginsenoside Ft1; Ucp, uncoupling protein; Wt, wild-type

1. Introduction

Obesity is a chronic and complex non-contagious medical condition characterized by excessive fat deposition in vital metabolic organs due to the disruption of lipid homeostasis[1]. It has been pathologically linked to a broad range of co-morbidities, including type 2 diabetes mellitus, non-alcoholic fatty liver diseases (NAFLD), hypertension, dyslipidemia, cardiovascular disease (CVD), as well as some cancers[2-5]. Obesity has been escalating global epidemic and more than 650 million adults (age≥18 years) around the world are diagnosed with obesity disorder in 2016[6]. The current conventional therapeutic options for the management of obesity include life-style interventions (exercise and diet) and pharmacotherapy. Recently, bariatric surgery becomes the most effective therapeutic intervention when all other treatments have failed[7]. However, surgery itself is invasive and has many side effects. Therefore, there is still an urgent need to develop innovative interventions and new policies to alleviate the detrimental effects of obesity by targeting metabolic regulators. Among the potential candidates, TGR5, a membrane-bound G protein-coupled bile acid (BA) receptor (also known as Gpbar-1), is a potent metabolic regulator and promising drug target[8-12].

TGR5 is ubiquitously expressed in immune cells and tissues of multiple metabolic organs, including intestine, liver, adipose tissue and muscle[13], and its involvement in various metabolic processes is crucial in regulation of the pathogenesis in metabolic disorders. Mechanistically, in brown adipose tissue (BAT) and muscle, the triggering of BA-induced TGR5 signaling promotes the production of energy expenditure through type 2 iodothyronine deiodinase (D2)-induced activation of thyroid hormone[14]. Interestingly, activation of TGR5 in enteroendocrine L-cells triggers the secretion of glucagon-like peptide-1 (GLP-1), which subsequently stimulates insulin secretion to alleviate glucose disorder, resulting in the improvement of pancreatic β-cell mass and glucose homeostasis[9,15]. Furthermore, activation of TGR5 in intestine also promotes the release of peptide tyrosine tyrosine (PYY) which attenuates food consumption rate[16]. On the other hand, TGR5 activation inhibits cytokine production by suppressing the nuclear factor

kappa-light-chain-enhancer of activated B cells (NF-κB) signaling pathway in activated macrophages[17]. These characteristics of TGR5 highlight it as a potential metabolic drug target. Since BAs have been reported as endogenous TGR5 ligands[11], cholic acid (CA)-derived 6α-ethyl-23(*S*)-methyl-CA (INT-777) was identified as a selective TGR5 agonist[18]. However, although INT-777 has been shown to exhibit potential therapeutic benefits in treating metabolic syndromes[18-20], severe side-effects have limited its further application in clinical trials[21-24]. Therefore, it is urgent to develop new TGR5 ligands with minimal adverse effects to treat obesity and its associated co-morbidities.

Radix Notoginseng, the dry roots of *Panax notoginseng* (Burk.) F.H. Chen (Araliaceae), has been used to cure trauma in traditional Chinese medicine for more than 2000 years[25]. One of the active compound notoginsenoside Ft1 (Ft1), separated from leaves and stems of *P. notoginseng*, is chemically a kind of saponin[26]. In the present study, we identified Ft1 as an agonist of the TGR5 by high-throughput screening of natural product libraries. We then evaluated the metabolic effects of Ft1 using diet-induced obese (DIO) model in mice. We also investigated the underlying mechanisms by which Ft1 improved lipid and glucose metabolism in DIO mice.

2. Materials and methods

2.1. Chemicals and reagents

Ft1 powder was provided by Shanghai R&D Center for Standardization of Chinese Medicines (Shanghai, China). Other chemicals including bile acids (BAs) were obtained from Sigma–Aldrich company (St. Louis, MO, USA), high fat diet (60 kcal% saturated HFD) and normal diet (chow diet, 10% kcal% derived from fat) were bought from Research Diet company (D12492 and D12450B, NJ, USA). FBS/ DMEM medium were obtained from Gibco, TG and TC measurement kits were from Wako Life Sciences.

2.2. Construction of Tgr5 stable expressed HEK293 cells

The cell line HEK293 was cultured in an incubator with 37 °C and 5% CO_2 by using Dulbecco's modified Eagle's medium (DMEM) with 10% fetal bovine serum. A plasmid expressed mouse *Tgr5* (pIRESneo3-m*Tgr5*) was transfected into HEK293 cells with Fugene 6 reagent. Forty-eight hours later, cells were treated with 500 mg/mL G418 and resistant cells were selected from them as previously described[27]. Resistant clones were evaluated by reverse transcription polymerase chain reaction (RT-PCR).

2.3. Tgr5 luciferase assay

To test whether Ft1 was a ligand of TGR5, the Luciferase Reporter Assay System (Promega Madison, WI, USA) was conducted as previously described[27]. The pCRE-luc reporter (50 ng), pCMV-galactosidase (5 ng) were transfected into *Tgr5* stable expressed HEK293 cells by using Fugene 6 reagent (Promega) for

18 h. The next day, cells were incubated with 0.2% DMSO as vehicle, INT-777 as positive control and Ft1 as indicated concentration for 24 h. Luciferase and *β*-galactosidase activities were measured 6 h later by employing Luciferase Assay System (Promega) and Galacto-Star (Applied Biosystems) reagents, respectively. *β*-Galactosidase was used as an internal control for normalization.

2.4. Adenosine 3′,5′ cyclic monophosphate (cAMP) secretion measurement

Tgr5 stable expressed HEK293 cells were incubated with 0.2% DMSO as vehicle or Ft1 for 30 min in serum-free Krebs Ringer buffer supplemented with 100 mmol/L Ro 20-1274 and 500 mmol/L 3-isobutyl-1-methylxanthine (IBMX, Sigma) and cAMP concentration were assayed in lysates by employing cAMP-Glo Assay Kit (Promega). Finally, cAMP levels were calculated by GraphPad Prism software with a cAMP standard curve.

2.5. Measurement of GLP-1 release from NCI-H716 cells

NCI-H716 cells from the American Type Culture Collection (ATCC) were maintained in suspension culture as described by the previously published methods[28]. To evaluated Ft1 mediated GLP-1 secretion, the cells were plated into 24-well culture plates precoated with Matrigel incubated for 48 h. Then cells were incubated with the Krebs-Ringer bicarbonate buffer (128.8 mmol/L NaCl, 4.8 mmol/L KCl, 1.2 mmol/L KH_2PO_4, 1.2 mmol/L $MgSO_4$, 2.5 mmol/L $CaCl_2$, 5 mmol/L $NaHCO_3$, 10 mmol/L HEPES, and 0.2% bovine serum albumin, pH 7.4) containing Ft1 (1, 5 and 10 μmol/L) or INT-777 as a positive control (10 μmol/L). After incubating at 37 °C for 2 h, the supernatants were collected and GLP-1 was measured by a GLP-1 active ELISA kit (Millipore).

2.6. Fxr transactivation assay

Caco-2 was differentiated as reported by Prof. Gonzalez's group[29]. Then Ft1 (10 μmol/L) supplemented with chenodeoxycholic acid (CDCA) (100 μmol/L) was exposed to differentiated Caco-2 cells for 24 h. All cell samples in each well were harvested for Realtime polymerase chain reaction (PCR) assay to determine mRNA levels of *Fxr* target genes.

Next, the transactivation of human *FXR* induced by Ft1 was evaluated. HEK293T cells were cotransfected with *EcRE-Luc*, ph*FXR*, ph*RXR* and *β*-galactosidase for 6 h using Fugene 6 reagent (Promega) as previous reported[30]. Then, the medium was replenished with fresh medium and Ft1 supplemented with GW4064 (5 μmol/L) was exposed to transfected HEK293T for 24 h in indicated concentrations. After treatment, cells were lysed to evaluate luciferase and *β*-galactosidase activities by employing Luciferase Assay System (Promega) and Galacto-Star (Applied Biosystems) reagents, respectively. *β*-Galactosidase was used as an internal control for normalization.

2.7. Animals and experimental design

C57BL/6 wild type (Wt) mice and *Cyp27a1* knockout (KO) mice (*Cyp27a1*$^{-/-}$, stock number, B6.129-*Cyp27a1*^{tm1Elt}/J) were obtained from the Jackson Laboratory (Bar Harbor, ME). *Tgr5*$^{-/-}$ mice in C57BL/6 background were kindly donated by Dr. Vassileva Galya as previously described[31]. Different kinds of genetic mice were kept at a pathogen-free animal facility under a standard 12 h:12 h light/dark cycle. All group mice were fed with standard chow diet and water *ad libitum*. NIH guidelines were followed by all procedures for the care and use of laboratory animals. The protocol of animal study has been accepted by City of Hope Institutional Animal Care and Use Committee (IACUC number: 13004). The general procedures of animal study were described as below. Six-week old male mice were fed with high-fat diet (D12492, 60% kcal from fat Research Diets, NJ, USA) for 8 weeks before performing the studies. Next, the obese mice were randomly divided into HFD group, Ft1 high dose group (HFD+Ft1-H, 100 g high fat diet supplemented with 100 mg Ft1, 100 mg/100 g diet) and Ft1 low dose group (HFD+Ft1-L, 100 g high fat diet supplemented with 50 mg Ft1, 50 mg/100 g diet) (*n*=8 per group). Mice fed with regular chow diet were used as control (*n*=8). Bodyweight and food intake were recorded for 6 weeks. For all experiments, age and body weight matched animals were used. After mice were euthanatized by CO_2, serum, liver, ileum, white adipose tissues (WAT) and BAT were collected and snap frozen in liquid nitrogen for RNA extracts, western blot analysis or biochemistry studies.

2.8. Analysis of endocrine hormones and metabolites

The Ultra Sensitive Mouse Insulin ELISA Kit (Crystal Chem Inc.) and portable glucose meter (Abbot Laboratories) were applied to measure fasting serum insulin levels and blood glucose level, respectively. At the 6th week following Ft1 treatment, all group mice were fasted for 14 h or 4 h and then intraperitoneally injected with D-glucose (2.0 g/kg bodyweight) or insulin (0.75 U/kg bodyweight) for glucose tolerance test (GTT) or insulin tolerance test (ITT), respectively. Blood from tails before and 15, 30, 60, or 120 min after the injection was collected for glucose levels test. 100 mg liver was homogenized in 1.0 mL PBS and 0.4 mL homogenate were used to extract hepatic lipids by using 3.2 mL $CHCl_3$-CH_3OH (chloroform/methanol, 2:1, *v*/*v*) mixture. Then, the lower organic phase was transferred and dried. The dried extract was resuspended in 1% Triton X-100 of absolute ethanol, and the triglyceride and cholesterol levels were measured with commercial kits (Wako Life Sciences). Serum glycerol was determined according to the instructions of commercial kits (Wako Life Sciences).

2.9. Measurement of GLP-1 release in vivo

Mice were orally treated with dipeptidyl-peptidase IV (DPP-IV) inhibitor sitagliptin (3 mg/kg) at 60 min

before the gavage with D-glucose (2.0 g/kg). Blood was collected by retro-orbital puncture in different indicated time points for the determination of plasma GLP-1 level. Serum GLP-1 levels were measured follow the instruction of commercial kits (Millipore).

2.10. Indirect calorimetry

Oxymax lab animal monitoring system (Columbus Instruments, Columbus, OH, USA) was employed to determine energy expenditures. After receiving Ft1 for 6 weeks, each group mice were kept in the separated metabolic chamber for 24 h to adapt the environment. Oxygen consumption volume (VO_2) and CO_2 release were determined during a 24 h period. Respiratory quotient (RQ) equals volumes of CO_2 production /volumes of O_2 consumption. Results are exhibited for the last 12 h of the light cycle and 12 h of the dark cycle over both dark and light phases.

2.11. Cold tolerance test

Each group mice were maintained in individual cages with food, and water which were placed in a 4 ℃ room. The cold tolerance was measured by placing the mice at 4 ℃ room for 3 h. Mouse rectal body temperatures were measured using a Thermo Scan thermometer (PRO 4000, Braun) prior to or at 60 min, 120 and 180 min after cold exposure.

2.12. BAs composition analysis

BAs composition was detected by ultra performance liquid chromatography–mass spectrometry as previously reported[32]. Serum BAs were extracted using 75% methanol. Specifically, 150 μL methanol was added to 50 μL serum and mixed by vortexing. Next, samples were centrifuged at 20,000×*g* (4 ℃) for 10 min. All the supernatant was separated and dried. Residues were reconstituted in 100 μL methanol–water (55:45, *v*/*v*; containing a mixture of 5 mmol/L ammonium acetate and 0.1% formic acid) before analysis.

2.13. Histological examination of liver and adipose tissues

When animal feeding was terminated, all mice were euthanized. Liver, BAT and WAT were fixed in 10% formalin, dehydrated and embedded in paraffin. Hematoxylin & eosin staining was performed for standard histological examination. 0.5% oil red O solution and Mayer's hematoxylin solution were used to stain frozen liver sections. Images were taken by employing Olympus BX51TF microscope (Olympus). Adipocyte size was quantified using Fiji Adiposoft software16 (Bethesda).

2.14. Quantitative real-time reverse transcription polymerase chain reaction (RT-PCR)

The liver, inguinal white adipose tissue (iWAT) and BAT were collected at 6th weeks post Ft1 treatment and total RNA from those tissues were extracted by using Trizol reagent (Molecular Research Center). After RNA quantification, 2 μg total RNA was transcripted reversely into cDNA by employing Superscript first-strand synthesis system (Invitrogen). Relative expressions of amplificants were measured with SYBR Green Supermix (Invitrogen) on an Applied Biosystems 7300 Real-Time PCR System (Applied Biosystems). Primer pairs used for gene determination were displayed in Supporting Information Tables S1 and S2. The relative mRNA levels of test genes were normalized with the internal control M36B4 or glyceraldehyde 3-phosphate dehydrogenase (*GAPDH*) by using the Applied Biosystems software.

2.15. Western blot analysis

The iWAT protein was extracted with tissue lysis buffer (Pierce). Samples were performed with Western blot analysis by incubating antibodies against HSL (Cell Signaling, #4107), pHSL (Cell Signaling, #4126), phospho-protein kinase A (pPKA) substrate (Cell Signaling, #9624) and GAPDH (Cell Signaling, #5174) using standard methodology. Western blotting was conducted and quantified with ImageJ software package as previously described[27].

2.16. Immunofluorescent staining

BAT and iWAT frozen sections were permeabilized by using PBS–0.05% Tx-100 solution for 30 min. Adipose tissue sections were incubated with uncoupling protein1 (UCP1, abcam, #ab225490) as the primary antibodies and washed 3 times with 1% BSA for 10 min after blocking. Next, secondary anti-rabbit antibodies were used for immunofluorescence. Finally, all sections were incubated for 15 min with 4′,6-diamidino-2-phenylindole (DAPI) for nuclei staining. Sections were mounted with VECTASHIELD (Vector Laboratories) and covered with slips after washing for 3 times. Images were taken with a scanning microscope (EVOS FL Auto, Thermo Scientific).

2.17. Statistical analysis

All data are presented as mean ± standard deviation (SD) or mean ± standard error (of estimate mean value) (SEM). The differences among two groups were compared by using Student's *t*-test (unpaired, two tailed). The differences among multiple groups were compared by using one-way analysis of variance (ANOVA) with Dunnett's *post hoc* test, while those tests were conducted only if F achieved $P<0.05$ and there was no significant variance inhomogeneity. Statistical analysis was undertaken only when each group size possesses a minimum of at $n=5$ independent samples. Data were analyzed using Prism (GraphPad, San Diego, CA, USA) software. The threshold of statistical significance was set at $P<0.05$.

3. Results

3.1. Ft1 ameliorates diet-induced obesity in mice

Tgr5 stable expression cell line was employed to whether Ft1 (Fig. 1A) was a *Tgr5* ligand *in vitro*. The results demonstrate that Ft1 activated *Tgr5* at 5 and 10 μmol/L test concentrations (Fig. 1B). Consistently, Ft1 at concentrations of 5 and 10 μmol/L remarkably stimulated cAMP secretion (Fig. 1C) and GLP-1 release *in vitro* (Supporting Information Fig. S1C) without any cytotoxicity (Fig. S1A and S1D). Since TGR5 regulates multiple signaling pathways to confer the metabolic homeostasis of lipids and glucose, we therefore investigated the pharmacological effects of Ft1 in DIO mice *in vivo*. A cohort of *Tgr5*$^{-/-}$ mice (KO) and wild-type mice were treated with HFD for eight weeks to induce diet-induced obesity. Then, HFD or HFD supplemented with Ft1 (100 mg/100 g diet or 50 mg/100 g diet) were fed for additional 6 weeks, while another cohort of KO and Wt mice were fed with a chow diet (chow) for the same duration. During the treatment, no obvious toxicity of Ft1 was observed. The Ft1-treated group showed similar food intake capacity compared to HFD group (Fig. 1E). Interestingly, although the bodyweight of mice fed with high dose of Ft1-mixed diet was heavier than that of chow-fed Wt mice, they exhibited less body-weight gain than HFD-fed mice over the course of experiments (Fig. 1D), suggesting that Ft1 conferred resistance to diet-induced obesity in mice (Fig. 1D). In contrast, *Tgr5*$^{-/-}$ mice treated with Ft1 at both high and low doses showed a similar body-weight gain compared to HFD-fed *Tgr5*$^{-/-}$ mice (Fig. 1D), indicating that Ft1 attenuated the HFD-induced obesity in a *Tgr5*-dependent manner. In addition, the liver and the WAT weights were determined and morphological changes were evaluated for the extent of lipid accumulation in different metabolic organs. The results reveal reductions in liver and bodyweight ratio (Fig. 1F), epididymal white adipose tissue (eWAT) weights (Supporting Information Fig. S2A), iWAT (Fig. 1G), adipocyte size of eWAT and iWAT (Fig. S2B), hepatic triglyceride (TG) content (Fig. S2C) and total cholesterol levels (TC) (Fig. S2D), following Ft1 treatment. As expected, these changes were not observed in *Tgr5*$^{-/-}$ mice with Ft1 treatment (Fig. 1D–G and Supporting Information Fig. S2A–S2D). Histopathological analysis indicates that Ft1 reduced hepatic steatosis and adipocyte hypertrophy in Wt mice (Fig. 1H and Fig. S2E), but not in *Tgr5*$^{-/-}$ mice (Fig. 1H and Fig. S2E). These results together demonstrate that *Tgr5* is required to mediate Ft1-induced weight loss and fat mass decrease in diet-induced obesity.

Insert Fig. 1

3.2. Ft1 improves HFD-induced glucose disorder in mice

To determine the effects of Ft1 treatment on glucose metabolism, GTT and ITT were conducted in all

experimental groups. The DIO mice showed reduced glucose tolerance and insulin resistance compared to those of chow-fed mice. Ft1 treatment significantly improved glucose tolerance (Fig. 2A) and insulin resistance (Fig. 2C) in Wt, but not in *Tgr5*$^{-/-}$ obese mice (Fig. 2B and D). Moreover, the increased fasting blood glucose (Fig. 2E) and insulin levels (Fig. 2F) in Wt obese mice were markedly reduced by Ft1 treatment, but not in *Tgr5*$^{-/-}$ mice (Fig. 2E and F). Taken together, these results indicate that Ft1 improves glucose metabolism in DIO mice in a *Tgr5*-dependent manner.

Insert Fig. 2

3.3. Ft1 induces GLP-1 secretion and elevates energy expenditure of DIO mice by activating Tgr5

TGR5 plays a key role in modulating GLP-1 release in the intestine. Enhanced GLP-1secretion improves hyperglycemia by stimulating glucose-dependent secretion of insulin[9]. Previously, synthetic *Tgr5* agonist INT-777 has been shown to promote GLP-1 secretion in enteroendocrine L-cells, thereby improving the glucose tolerance in a *Tgr5*-dependent manner[9]. To test whether Ft1 could confer its metabolic benefits *via Tgr5*-induced GLP-1 secretion, oral glucose was loaded while tracing the plasma GLP-1 level. Notably, Ft1 treatment showed a strong increase of GLP-1 release in response to an oral glucose load (Fig. 3A). In *Tgr5*$^{-/-}$ mice, however, these responses were dramatically abolished (Fig. 3B), suggesting that *Tgr5* is required to mediate GLP-1 secretion. In order to investigate the impact of Ft1 on energy metabolism, we analyzed the rates of oxygen consumption and energy expenditure in mice. In Ft1-treated Wt mice, energy expenditure (Fig. 3C) was dramatically enhanced in the dark phases. The oxygen consumption (Fig. 3D) was also augmented in the dark phase compared to those of untreated Wt mice. The average energy expenditure (Fig. 3E) and oxygen consumption (Fig. 3F) in 24 h were significantly increased after Ft1 treatment. Taken together, these results suggest that the increase in energy expenditure may contribute to the reduced bodyweight gain in Wt mice that received Ft1. However, the promotion of energy expenditure induced by Ft1 was abolished in *Tgr5*$^{-/-}$ mice.

Insert Fig. 3

3.4. Ft1 promotes lipolysis and thermogenesis by activating Tgr5 in adipose tissues

To determine the potential mechanism governing the *Tgr5*-dependent decrease of weight loss perceived after Ft1 treatment, we examined a potential TGR5-cAMP-PKA pathway in inducing lipolysis in iWAT. The results demonstrated that Ft1 strongly increased the protein levels of PKA substrates and increased phosphorylation of HSL (Fig. 4A). Meanwhile, the serum glycerol level was significantly increased after Ft1 administration (Fig. 4B), suggesting that lipolysis was elevated in iWAT. We then measured the mRNA levels of thermogenesis-associated genes in iWAT and BAT. The results show that Ft1 significantly increased the levels of mRNAs encoding *Ucp1*, peroxisome proliferator-activated receptor-γ

coactivator-1α (*Pgc1a*), transcription factor PR domain containing 16 (*Prdm16*), and Kelch like family member 13 (*Klhl13*) in iWAT of Wt mice, but did not affect the mRNA levels of cytochrome *c* oxidase polypeptide 7A1 (*Cox7a1*), solute carrier family 27 member 1 (*Slc27a1*), tumor necrosis factor receptor superfamily member 5 (*Cd40*) and tumor necrosis factor receptor superfamily member 9 (*Cd137*) (Fig. 4C). Meanwhile, Ft1 significantly up-regulated the mRNA levels of *Pgc1a, Ucp1, Ucp3*, muscle-type carnitine palmitoyltransferase 1 *(Cpt1b)* and type 2 iodothyronine deiodinase (*Dio2*) rather than straight-chain acyl-CoA oxidase1 (*Acox1*) in the BAT (Fig. 4D) of Wt mice following Ft1 treatment. A similar profile of energy expenditure-associated gene expressions in both iWAT and BAT were observed in KO mice fed with or without Ft1. Immunofluorescence analysis further confirmed that UCP1 expression in both iWAT and BAT of Wt mice were increased after Ft1 administration. In contrast, no further increase was observed in *Tgr5*$^{-/-}$ mice fed with Ft1-mixed diet (Fig. 4E), suggesting that Ft1 might confer the increase in energy expenditure in DIO mice *via Tgr5* activation in adipose tissues.

Insert Fig. 4

3.5. Ft1 as a Fxr antagonist enhances hepatic BA synthesis in vivo

To test whether Ft1 could activate *Tgr5* directly to mediate the metabolic effects in DIO mice, we examined the tissue/organ distribution patterns of Ft1 in Wt mice. The results show that Ft1 was mainly distributed in various parts of the intestine tissues, including the ileum and colon (Supporting Information Fig. S3). The content of Ft1 was low in serum as well as the major metabolic organs, including liver, iWAT, eWAT, BAT and muscle (Fig. S3). These results indicate that Ft1 might mainly act in the intestine, but not in other metabolic organs. Because BAs are the endogenous *Tgr5* ligands, we thus measured the levels of BAs after Ft1 treatment to answer how Ft1 treatment could activate *Tgr5* in adipose tissues. Intriguingly, most serum tauro-conjugated and unconjugated BA levels were strongly increased in both Wt and *Tgr5*$^{-/-}$ mice (Fig. 5A and B), indicating that Ft1 increased BA levels in a *Tgr5*-independent manner. Although it has been reported that *TGR5* activation might affect BA synthesis, *Tgr5*-specific agonist INT777 did not show significant impact on BA production, whereas *Fxr* and *Tgr5* dual agonists could decrease BA secretion into the intestine[33]. To address the question of why BA levels were elevated after Ft1 treatment, the expressions of *Fxr* and its target genes in ileum and liver were determined. The results showed that *Fxr* transcriptional activity was suppressed as indicated by the reduced expressions of *Fxr* target genes, including intestinal bile acid-binding protein (*Ibabp*), the small heterodimer partner (*Shp*) and fibroblast growth factor 15 (*Fgf15*) in the ileum (Fig. 5C). We also observed a down-regulated FGF15 protein level in serum (Fig. 5D), which might result in the upregulated levels of hepatic *Cyp7a1* and *Cyp27a1* genes (Fig. 5E), two key enzymes of BA synthesis in the liver. Consistently, the results of

luciferase assay confirm that the transactivation of *Fxr* was significantly suppressed in a dose-dependent manner by Ft1 treatment (Fig. 5F). Consistently, when Caco-2 cells were treated with Ft1 for 24 h, we observed a significant decrease in the mRNA expressions of *FXR* target genes, including *SHP*, *FGF19* and intestinal bile acid-binding protein (*IBABP*) (Fig. 5G–I).

Insert Fig. 5

3.6. The metabolic benefits conferred by Ft1 are abolished in Cyp27a1$^{-/-}$ mice

To further test whether the metabolic benefits exerted by Ft1 were indeed mediated by BA elevation, we examined the metabolic effects of Ft1 in *Cyp27a1*$^{-/-}$ mice with a markedly reduced BA pool. Wt and *Cyp27a1*$^{-/-}$ mice were fed with HFD, and then treated with Ft1-mixed diet. Ft1 had no effect on food intake rate in both Wt and *Cyp27a1*$^{-/-}$ mice compared to that of HFD fed group (Fig. 6A). As expected, Ft1 failed to induce further weight loss in *Cyp27a1*$^{-/-}$ mice (Fig. 6A). At 6 weeks after Ft1 treatment, we assessed the weight of eWAT (Fig. S4A) and iWAT (Fig. 6B), adipocyte size of eWAT and iWAT (Fig. S4C), as well as measured liver/body weight ratio (Fig. 6B). We also performed a histopathological analysis for adipocyte hypertrophy (Fig. 6D and Fig. S4D). As expected, the values of these parameters from HFD group were similar to those of Ft1 treatment group of *Cyp27a1*$^{-/-}$ mice. Ft1 could not further improve the metabolic phenotypes, including hepatosteatosis in *Cyp27a1*$^{-/-}$ mice (Fig. 6B, C, and Fig. S4D). Similar results were also observed for fasting blood glucose level, glucose toleranceand insulin sensitivity (Fig. S4B, Fig. 6E and F). Altogether, these results confirm that *Cyp27a1* deletion abolished the metabolic effects of Ft1 due to a markedly lower level of BA pool.

Insert Fig. 6

To verify whether the endogenous BAs were the key mediators for activation of *Tgr5* signaling following Ft1 treatment, we then evaluated the effects of GLP-1 secretion and thermogenesis in *Cyp27a1*$^{-/-}$ mice treated with Ft1. The data show that Ft1 could still promote the GLP-1 secretion after oral glucose load in both Wt and *Cyp27a1*$^{-/-}$ mice (Fig. 7A), indicating that Ft1 could directly promote GLP-1 secretion due to its high distribution in the intestine. However, Ft1 administration failed to increase the serum levels of most of the BA species in *Cyp27a1*$^{-/-}$ mice (Fig. 7B). Furthermore, the augmentation of pHSL-induced lipolysis as well as serum glycerol level in iWAT after Ft1 treatment were not detected in *Cyp27a1*$^{-/-}$ mice (Fig. 7C and D), suggesting that Ft1 induced lipolysis through BAs. Besides, Ft1 increased the body temperature of Wt mice rather than *Cyp27a1*$^{-/-}$ mice after cold exposure for 3 h (Fig. 7E). The upregulated expressions of thermogenesis-associated genes after Ft1 treatment were abolished in *Cyp27a1*$^{-/-}$ mice (Fig. 7F), further confirming that Ft1 conferred the increased energy expenditure in DIO mice through BA-dependent *Tgr5* activation in adipose tissues.

Insert Fig. 7

4. Discussion

Functional activation of *TGR5* promotes rapid intracellular cAMP production, leading to sequential downstream reactions to regulate various metabolic processes[34]. Our previous findings demonstrated that vertical sleeve gastrectomy, which is the most effective approach for morbid obesity, imparts its metabolic benefits through BA-mediated TGR5 activation[34]. TGR5 is a promising drug target to develop new therapeutic agents for treating obesity and associated co-morbidities. We screened a series of natural products from compound libraries and identified Ft1 as a potent TGR5 ligand *in vitro*. Although *in vivo* animal data demonstrated that Ft1 enhanced GLP-1 secretion through intestinal *Tgr5* activation, it did not activate *Tgr5* directly in adipose tissue. Instead, Ft1 acts as a *Fxr* antagonist in the intestine, which led to increased hepatic BA production and serum BA levels to activate *Tgr5* in adipose tissues.

BAs are synthesized from cholesterol in the liver parenchymal cells[35]. During digestion, they act as surfactants to emulsify dietary fat and facilitate intestinal absorption of lipids, cholesterol, and a number of vitamins[36]. Currently, the functions of BAs are revealed as signaling molecules that impart systemic changes in metabolism via targeting nuclear receptor *Fxr*[37,38] and cell surface receptor *Tgr5*[39]. *Fxr* is the primary BA receptor to control BA synthesis in the liver. *Tgr5* is also considered to modulate hepatic BA production to some extent. *Tgr5* gene ablation significantly increases taurocholic acid (TCA) and taurodeoxycholic acid (TDCA) levels and blunts the generation of tauro α-muricholic acid (TαMCA) and tauro β-muricholic acid (TβMCA) in both free-fed and fasting states compared to Wt mice, which are consistent with our data[40]. However, in the present study, we observed that Ft1 alters BA production mainly through the suppression of intestinal *Fxr*. The downregulation of intestinal *Fxr* target genes and the reduced serum level of FGF15 support this hypothesis. TGR5 has been demonstrated as an endogenous BA receptor by Dr. Tanaka's group[41]. In this context, taurolithocholic acid (TLCA) and lithocholic acid (LCA) are the most potent *Tgr5* ligands, CA, DCA, CDCA and their tauro-conjugated products also show TGR5 activation effects[42]. Currently, TGR5 has been manifested as the downstream effector in BA signaling pathway to regulate various metabolic processes[13]. Pharmacological activation of TGR5 by agonists or genetic overexpression of the receptor itself imparts beneficial effects on the regulation of glucose and lipid metabolism[9,43]. However, under normal conditions, serum BA levels are typically low. Here we demonstrate that Ft1 can significantly enhance hepatic BA production and increase serum BA levels to exert metabolic benefits in DIO mice *via Tgr5* activation.

It is well documented that traditional Chinese herbal medicines are generally administered orally, because many constituents could not be absorbed into peripheral blood circulation due to the low bioavailability[44]. For instance, the bioavailability of berberine is less than 1%, but it still significantly imparts metabolic improvement of non-alcoholic fatty liver diseases (NAFLD) animal models by directly affecting gut microbiota and intestinal-liver signaling[45]. Another particular example is the saponins,

which are the major active compounds from ginseng and *Panax notoginseng*. It has been reported that deglycosylation and hydroxylation are the major metabolic pathway for saponins in the intestine[46]. Aglycone of Ft1 is protopanaxatriol (PPT), which did not show effects on *Tgr5* activation (Fig. S1B). Therefore, the direct target tissue of Ft1 may be the intestine rather than other metabolic tissues. The intestine has been considered as a major endocrinal organ and immune organrather than an organ just for digestion and absorption[47,48]. Multiple functional metabolites can be produced in the intestine and absorbed into blood circulation to execute the metabolic functions. For example, short chain fatty acids SCFA and branched chain amino acid (BCAA) are now known as functional metabolites to regulate metabolism[49,50]. Intestine also produces a variety of gut hormones including FGF15, GLP-1, polypeptide YY (PYY) and glucose-dependent insulinotropic peptide (GIP) to regulate different metabolic functions[51]. Here we showed that Ft1 upregulated expressions of *Cyp7a1* and *Cyp27a1* in liver, two key enzymes in the classic and alternative pathways of BA synthesis by suppressing the transcriptionl activation of intestinal *Fxr*. Indeed, the inhibition of intestinal *Fxr* conferred metabolic benefit for HFD-induced obese and insulin resistance mice[29,52,53]. Similarly, the metabolic disorders of HFD-fed hamsters were improved through T*β*-MCA mediated suppression of intestinal FXR following gut microbiota depletion[54]. It is noteworthy that the diabetic mouse treated with hyocholicacid (HCA) promotes GLP-1 secretion and improve glucose homeostasis by activating *Tgr5* and inhibiting *Fxr*[55], indicating that it might be a promising approach to develop dual *Tgr5* agonist and *Fxr* antagonist for treatment of diabetes. Our data also has proved that Ft1 as a single compound with opposite activities on two key BA receptors alleviated high fat diet-induced obesity and insulin resistance in mice.

5. Conclusions

Our present studies demonstrated that Ft1 is a *Tgr5* agonist but *Fxr* antagonist to alleviate high fat diet-induced obesity and insulin resistance in mice. On one hand, Ft1 activates intestinal *Tgr5* to enhance intestinal GLP-1 release. On the other hand, Ft1 increases the hepatic BA production by suppressing intestinal *Fxr*. The elevated serum BA levels subsequently activate *Tgr5* in adipose tissues to increase energy expenditure, thereby conferring beneficial metabolic effects in obese mice (Fig. 8). Ft1 thus may represent an innovative compound with opposing effects on two key BA receptors and may be a potential leading compound for anti-diabetes drug development.

Insert Fig. 8

Acknowledgments

This work is financially sponsored by Shanghai Pujiang Program (17PJ1408800, China) and the Natural Science Foundations of China to Lili Ding (81773961), Zhengtao Wang (81920108033) and Yingbo

Yang (81703682). It is also financially supported by the National S&T Major Special Projects of China (No. 2017ZX09309006) to Li Yang and Interdisciplinary Program of Shanghai Jiao Tong University to Qiaoling Yang (YG2019QNA03, China). This work is partially supported by R01DK124627, George Schaeffer fund and John Hench fund (USA) to Wendong Huang. We thank Tongxi Zhuang and Suzhou BioNovoGene Metabolomics Platform (Suzhou, China) for providing material to draw the graphical abstract.

Author contributions

Wendong Huang, Li Yang, Lili Ding and Zhengtao Wang designed the experiments and secured funding. Lili Ding, Qiaoling Yang, Eryun Zhang, Siming Sun, Yangmeng Wang and Linshan Jiang performed the experiments. Lili Ding, Yingbo Yang, Tong Tian, Zhengcai Ju and Xunjiang Wang analyzed the data. Lili Ding wrote the manuscript. Wendong Huang provided editing and final approval of the manuscript.

Conflicts of interest

The authors have no conflicts of interest to declare.

References

1. Sikaris KA. The clinical biochemistry of obesity. *Clin Biochem Rev* 2004;**25**:165-81.
2. Calle EE, Rodriguez C, Walker-Thurmond K, Thun MJ. Overweight, obesity, and mortality from cancer in a prospectively studied cohort of U.S. adults. *N Engl J Med* 2003;**348**:1625-38.
3. Fruh SM. Obesity: risk factors, complications, and strategies for sustainable long-term weight management. *J Am Assoc Nurse Pract* 2017;**29**:S3-14.
4. Lakhani HV, Sharma D, Dodrill MW, Nawab A, Sharma N, Cottrill CL, et al. Phenotypic alteration of hepatocytes in non-alcoholic fatty liver disease. *Int J Med Sci* 2018;**15**:1591-9.
5. Dădârlat-Pop A, Sitar-Tăut A, Zdrenghea D, Caloian B, Tomoaia R, Pop D, et al. Profile of obesity and comorbidities in elderly patients with heart failure. *Clin Interv Aging* 2020;**15**:547-56.
6.World Health Organization. Obesity and overweight. World Health Organization. 2020. Available from: https://www.who.int/news-room/fact-sheets/detail/obesity-and-overweight
7. Cefalu WT, Bray GA, Home PD, Garvey WT, Klein S, Pi-Sunyer FX, et al. Advances in the science, treatment, and prevention of the disease of obesity: reflections from a Diabetes Care Editors' Expert Forum. *Diabetes Care* 2015;**38**:1567-82.
8. Chen X, Lou G, Meng Z, Huang W. TGR5: a novel target for weight maintenance and glucose metabolism. *Exp Diabetes Res* 2011;**2011**:853501.

9. Thomas C, Gioiello A, Noriega L, Strehle A, Oury J, Rizzo G, et al. TGR5-mediated bile acid sensing controls glucose homeostasis. *Cell Metab* 2009;**10**:167-77.
10. Velazquez-Villegas LA, Perino A, Lemos V, Zietak M, Nomura M, Pols TWH, et al. TGR5 signalling promotes mitochondrial fission and beige remodelling of white adipose tissue. *Nat Commun* 2018;**9**:245.
11. Maruyama T, Miyamoto Y, Nakamura T, Tamai Y, Okada H, Sugiyama E, et al. Identification of membrane-type receptor for bile acids (M-BAR). *BiochemBiophys Res Commun* 2002;**298**:714-19.
12. Li T, Chiang JY. Bile acid signaling in metabolic disease and drug therapy. *Pharmacol Rev* 2014;**66**:948-83.
13. Duboc H, Taché Y, Hofmann AF. The bile acid TGR5 membrane receptor: from basic research to clinical application. *Dig Liver Dis* 2014;**46**:302-12.
14. Watanabe M, Houten SM, Mataki C, Christoffolete MA, Kim BW, Sato H, et al. Bile acids induce energy expenditure by promoting intracellular thyroid hormone activation. *Nature* 2006;**439**:484-9.
15. Kuhre RE, Holst JJ, Kappe C. The regulation of function, growth and survival of GLP-1-producing L-cells. *Clin Sci (Lond)* 2016;**130**:79-91.
16. Bala V, Rajagopal S, Kumar DP, Nalli AD, Mahavadi S, Sanyal AJ, et al. Release of GLP-1 and PYY in response to the activation of G protein-coupled bile acid receptor TGR5 is mediated by Epac/PLC-ε pathway and modulated by endogenous H2S. *Front Physiol* 2014;**5**:420.
17. Wang YD, Chen WD, Yu D, Forman BM, Huang W. The G-protein-coupled bile acid receptor, Gpbar1 (TGR5), negatively regulates hepatic inflammatory response through antagonizing nuclear factor κ light-chain enhancer of activated B cells (NF-κB) in mice. *Hepatology* 2011;**54**:1421-32.
18. Pellicciari R, Gioiello A, Macchiarulo A, Thomas C, Rosatelli E, Natalini B, et al. Discovery of 6alpha-ethyl-23(*S*)-methylcholic acid (S-EMCA, INT-777) as a potent and selective agonist for the TGR5 receptor, a novel target for diabesity. *J Med Chem* 2009;**52**:7958-61.
19. Guo C, Chen WD, Wang YD. TGR5, not only a metabolic regulator. *Front Physiol* 2016;**7**:646.
20. Hegade VS, Speight RA, Etherington RE, Jones DE. Novel bile acid therapeutics for the treatment of chronic liver diseases. *Therap Adv Gastroenterol* 2016;**9**:376-91.
21. Fiorucci S, Distrutti E, Ricci P, Giuliano V, Donini A, Baldelli F. Targeting FXR in cholestasis: hype or hope. *Expert OpinTher Targets* 2014;**18**:1449-59.
22. Lavoie B, Balemba OB, Godfrey C, Watson CA, Vassileva G, Corvera CU, et al. Hydrophobic bile salts inhibit gallbladder smooth muscle function *via* stimulation of GPBAR1 receptors and activation of KATP channels. *J Physiol* 2010;**588**:3295-305.

23. Stepanov V, Stankov K, Mikov M. The bile acid membrane receptor TGR5: a novel pharmacological target in metabolic, inflammatory and neoplastic disorders. *J Recept Signal Transduct Res* 2013;**33**:213-23.

24. Fryer RM, Ng KJ, Nodop Mazurek SG, Patnaude L, Skow DJ, Muthukumarana A, et al. G protein-coupled bile acid receptor 1 stimulation mediates arterial vasodilation through a K(Ca)1.1 (BK(Ca))-dependent mechanism. *J Pharmacol Exp Ther* 2014;**348**:421-31.

25. Chen QS. Pharmacological studies on notoginseng saponins isolated from the fibrous root of *Panax notoginseng*. *Bull Chin Mater Med* 1987;**12**:45-7.

26. Chen JT, Li HZ, Wang D, Zhang YJ, Yang CR. New dammarane monodesmosides from the acidic deglycosylation of *notoginseng*-leaf saponins. *Helv Chim Acta* 2006;**89**:1442-8.

27. LouGY, Ma XX, Fu XH, Meng ZP, Zhang WY, Wang YD, et al. GPBAR1/TGR5 mediates bile acid-induced cytokine expression in murine Kupffer cells. *PLoS One* 2014;**9**:e93567.

28. Reimer RA, Darimont C, Gremlich S, Nicolas-Metral V, Ruegg UT, Mace K. A human cellular model for studying the regulation of glucagon-like peptide-1 secretion. *Endocrinology* 2001;**142**:4522-8.

29. Jiang C, Xie C, Lv Y, Li J, Krausz KW, Shi J, et al. Intestine-selective farnesoid X receptor inhibition improves obesity-related metabolic dysfunction. *Nat Commun* 2015;**6**:10166.

30.Ding L, Zhang B, Li J, Yang L, Wang Z. Beneficial effect of resveratrol on α-naphthyl isothiocyanate-induced cholestasis *via* regulation of the FXR pathway. *Mol Med Rep* 2018;**17**:1863-72.

31. Vassileva G, Golovko A, Markowitz L, Abbondanzo SJ, Zeng M, Yang S, et al. Targeted deletion of Gpbar1 protects mice from cholesterol gallstone formation. *Biochem J* 2006;**398**:423-30.

32. Yang L, Xiong A, He Y, Wang Z, Wang C, Wang Z, et al. Bile acids metabonomics study on the CCl_4- and α-naphthylisothiocyanate-induced animal models: quantitative analysis of 22 bile acids by ultraperformance lipid chromatography-mass spectrometry. *Chem Res Toxicol* 2008;**21**: 2280-8.

33. Donepudi AC, Boehme S, Li F, Chiang JY. G protein-coupled bile acid receptor plays a key role in bile acid metabolism and fasting-induced hepatic steatosis. *Hepatology* 2017; **65**: 813-27.

34. Pols TW, Noriega LG, Nomura M, Auwerx J, Schoonjans K. The bile acid membrane receptor TGR5 as an emerging target in metabolism and inflammation. *J Hepatol* 2011;**54**:1263-72.

35. Chiang JY. Regulation of bile acid synthesis. *Front Biosci* 1998;**3**:d176-93.

36. Monte MJ, Marin JJ, Antelo A, Vazquez-Tato J. Bile acids: chemistry, physiology, and pathophysiology. *World J Gastroenterol* 2009;**15**:804-16.

37. Wang H, Chen J, Hollister K, Sowers LC, Forman BM. Endogenous bile acids are ligands for the nuclear receptor FXR/BAR. *Mol Cell* 1999;**3**:543-53.

38. Parks DJ, Blanchard SG, Bledsoe RK, Chandra G, Consler TG, Kliewer SA, et al. Bile acids: natural ligands for an orphan nuclear receptor. *Science* 1999;**284**:1365-8.

39.Staels B, Fonseca VA. Bile acids and metabolic regulation: mechanisms and clinical responses to bile acid sequestration. *Diabetes Care* 2009;**32 Suppl 2**:S237-45.

40. Maruyama T, Tanaka K, Suzuki J, Miyoshi H, Harada N, Nakamura T, et al. Targeted disruption of G protein-coupled bile acid receptor 1 (Gpbar1/M-Bar) in mice. *J Endocrinol* 2006; **191**: 197-205.

41. Maruyama T, Miyamoto Y, Nakamura T, Tamai Y, Okada H, Sugiyama E, et al. Identification of membrane-type receptor for bile acids (M-BAR). *Biochem Biophys Res Commun* 2002; **298**:714-9.

42. Ding LL, Yang L, Wang ZT, Huang WD. Bile acid nuclear receptor FXR and digestive system diseases. *Acta Pharm Sin B* 2015; **5**: 135-44.

43. Finn PD, Rodriguez D, Kohler J, Jiang Z, Wan S, Blanco E, et al. Intestinal TGR5 agonism improves hepatic steatosis and insulin sensitivity in Western diet-fed mice. *Am J Physiol Gastrointest Liver Physiol* 2019;**316**:G412-24.

44. Suroowan S, Mahomoodally MF. Herbal medicine of the 21st century: a focus on the chemistry, pharmacokinetics and toxicity of five widely advocated phytotherapies. *Curr Top Med Chem* 2019;**19**:2718-38.

45. Yan TT, Yan NN, Wang P, Xia YL, Hao HP, Wang GJ, et al. Herbal drug discovery for the treatment of nonalcoholic fatty liver disease. *Acta Pharm Sin B* 2020;**10**:3-18.

46. He Y, Hu Z, Li A, Zhu Z, Yang N, Ying Z, et al. Recent advances in biotransformation of saponins. *Molecules* 2019;**24**:2365.

47. Chassaing B, Kumar M, Baker MT, Singh V, Vijay-Kumar M. Mammalian gut immunity. *Biomed J* 2014;**37**:246-58.

48. Sinagoga KL, Wells JM. Generating human intestinal tissues from pluripotent stem cells to study development and disease. *EMBO J* 2015;**34**:1149-63.

49. Tajiri K, Shimizu Y. Branched-chain amino acids in liver diseases. *Transl Gastroenterol Hepatol* 2018;**3**:47.

50. Qi XY, Yun CY, Sun LL, Xia JL, Wu Q, Wang Y, et al. Gut microbiota-bile acid-interleukin-22 axis orchestrates polycystic ovary syndrome. *Nat Med* 2019;**25**:1225-33.

51. Martin AM, Sun EW, Keating DJ. Mechanisms controlling hormone secretion in human gut and its relevance to metabolism. *J Endocrinol* 2019;**244**:R1-15.

52. Sun L, Xie C, Wang G, Wu Y, Wu Q, Wang X, et al. Gut microbiota and intestinal FXR mediate the clinical benefits of metformin. *Nat Med* 2018;**24**:1919-29.

53. Gonzalez FJ, Jiang CT, Patterson AD. An intestinal microbiota-farnesoid X receptor axis modulates metabolic disease. *Gastroenterology* 2016;**151**:845-59.

54. Sun LL, Pang YY, Wang XM, Wu Q, Liu HY, Liu B, et al. Ablation of gut microbiota alleviates obesity-induced hepatic steatosis and glucose intolerance by modulating bile acid metabolism in hamsters. *Acta Pharm Sin B* 2019;**9**:702-710.
55. Zheng XJ, Chen TL, Jiang RQ, Zhao AH, Wu Q, Kuang JL, et al. Hyocholic acid species improve glucose homeostasis through a distinct TGR5 and FXR signaling mechanism. *Cell Metabolism* 2020. Available from: https://doi.org/10.1016/j.cmet.2020.11.017.

Figure captions

Figure 1 Ft1 improves body weight and hepatic steatohepatitis of DIO mice through activation of *Tgr5*. (A) Chemical structure of Ft1. (B) *Tgr5* luciferase reporter activities of Ft1. (C) cAMP elicited by Ft1 after binding to the *TGR5* and intracellular cAMP levels were measured by luminescence. Wt and *Tgr5*$^{-/-}$ (KO) mice were fed with HFD to induce obesity, and then treated with Ft1 for 6 weeks. (D) Body weight and (E) food intake of Wt and *Tgr5*$^{-/-}$ mice after Ft1 treatment. (F) Liver/bodyweight ratio, (G) iWAT weight and (H) oil red staining of liver sections and H&E staining of iWAT sections in both Wt and *Tgr5*$^{-/-}$ mice at 6th week after Ft1 treatment. Values are mean±SD (n=6 per group), $^{*}P$<0.05, $^{**}P$<0.01 *vs.* vehicle by two tailed Student's *t* test for panels A–C. Values are mean±SEM (n=8 per group), $^{*}P$<0.05, $^{**}P$<0.01 *vs.* HFD group by one-way ANOVA with Dunnett's post-test for panels D–G. Scale bar, 100 μm.

Figure 2 Ft1 mediated improvement of glucose homeostasis in DIO mice is dependent on *Tgr5*. GTT at time point of 0 to 120 min and area under the curve (AUC) of (A) Wt and (B) *Tgr5*$^{-/-}$ mice after intraperitoneal (ip) injection with 2.0 g/kg D-glucose, ITT at time point 0 to 120 min and area under curve (AUC) of (C) Wt and (D) *Tgr5*$^{-/-}$ KO mice after ip injection with 0.75 U/kg insulin. (E) Fasting blood glucose levels and (F) blood insulin levels of Wt and *Tgr5*$^{-/-}$ mice at 6 weeks after Ft1 treatment. Values are mean±SEM (n=8 per group), $^{*}P$<0.05, $^{**}P$<0.01 *vs*. HFD group by one-way ANOVA with Dunnett's post-test.

Figure 3 Ft1 induces GLP-1 secretion and increases energy expenditure of DIO mice by activation of *Tgr5*. GLP-1 production and the AUC of (A) Wt and (B) *Tgr5*$^{-/-}$ mice. (C) Energy expenditure over 24 h period, (D) O_2 consumption over light phase and dark phase, (E) the average energy expenditure, and (F) the average oxygen consumption over 24 h period in Wt and *Tgr5*$^{-/-}$ mice at 6th week after Ft1 treatment. Values are mean±SEM (n=6 per group), $^{*}P$<0.05, $^{**}P$<0.01 *vs*. HFD group by one-way ANOVA with Dunnett's post-test.

Figure 4 Ft1 promotes lipolysis and thermogenesis in DIO mice through activation of *Tgr5*. (A) The protein amounts of PKA substrates, HSL and phosphorylation of HSL in inguinal fat of Wt and *Tgr5*$^{-/-}$ mice after Ft1 administration. (B) Blood glycerol level of Wt and *Tgr5*$^{-/-}$ mice after Ft1 treatment. The mRNA levels of energy expenditure associated genes in (C) iWAT and (D) BAT of Wt and *Tgr5*$^{-/-}$ mice after Ft1 treatment. (E) UCP1 immunofluorescence staining of iWAT and BAT sections from Wt and *Tgr5*$^{-/-}$ mice treated with Ft1. Blue, DAPI; Green, UCP1. Scale bar, 100 μm. Values are mean±SEM

(*n*=5–6 per group), $^{*}P<0.05$, $^{**}P<0.01$ *vs.* HFD group by one-way ANOVA with Dunnett's post-test.

Figure 5 Ft1 is an *Fxr* antagonist and enhances hepatic bile acids synthesis in DIO mice. (A) Taurine-conjugated BAs, glycine-conjugated BAs, unconjugated BAs and (B) total BAs in serum of Wt and *Tgr5*$^{-/-}$ mice after Ft1 treatment. (C) Relative mRNA expression of *Fxr* and its target genes in ileum, (D) serum *FGF15* amounts and (E) relative mRNA expressions of *Fxr* and its target genes in liver of Wt and *Tgr5*$^{-/-}$ mice after Ft1 treatment. (F) Luciferase activity were assayed, (G) *SHP*, (H) *FGF19* and (I) *IBABP* mRNA expressions of differentiated Caco2 cells after treatment with 100 μmol/L CDCA with 10μmol/L Ft1, expression was normalized to *GAPDH* mRNA. Values are mean ± SD (*n*=5–6 per group), $^{**}P<0.01$ compared to vehicle, $^{\#}P<0.05$ compared to GW4064 by two tailed Student's *t* test for panels F–I. Values are mean±SEM (*n*=8 per group), $^{*}P<0.05$, $^{**}P<0.01$ *vs.* HFD group by one-way ANOVA with Dunnett's post-test for panels A–E.

Figure 6 The metabolic benefits induced by Ft1 are lost in *Cyp27a1*$^{-/-}$ mice. Wt and *Cyp27a1*$^{-/-}$ mice were fed with HFD to lead obesity, and then treated with Ft1 for additional 6 weeks. (A) Body weight and food intake of Wt and *Cyp27a1*$^{-/-}$ mice after Ft1 treatment. (B) Liver/bodyweight ratio, iWAT weight of both Wt and *Tgr5*$^{-/-}$ mice at 6th week after Ft1 treatment. (C) Oil red staining of liver sections and (D) H&E staining of iWAT sections from Wt and *Tgr5*$^{-/-}$ mice at 6 weeks after Ft1 treatment. (E) IPGTT curve during 0 to 120 min and AUC of Wt and *Cyp27a1*$^{-/-}$ mice after ip injection with 2.0 g/kg D-glucose, (F) IPITT curve during 0 to 120 min and AUC of Wt and *Cyp27a1*$^{-/-}$ mice after ip injection with 0.75 U/kg insulin. Values are mean±SEM (*n*=8 per group), $^{*}P<0.05$, $^{**}P<0.01$ *vs.* HFD group by one-way ANOVA with Dunnett's post-test. Scale bar, 100 μm.

Figure 7 Ft1 mediated thermogenesis is abolished in *Cyp27a1*$^{-/-}$ mice. (A) GLP-1 release at indicated time point and AUC of Wt and *Cyp27a1*$^{-/-}$ mice. (B) BAs profile in WT and *Cyp27a1*$^{-/-}$ mice after Ft1 treatment. (C) The protein amounts of HSL and phosphorylation of HSL in inguinal fat of Wt and *Tgr5*$^{-/-}$ mice after Ft1 administration. (D) Blood glycerol level of Wt and *Cyp27a1*$^{-/-}$ mice after Ft1 treatment. (E) Cold intolerance in Wt and *Cyp27a1*$^{-/-}$ mice was measured before and at 1, 2, and 3 h after cold exposure (4 °C), mouse rectal body temperatures were measured using a ThermoScan thermometer. (F) Energy expenditure associated genes in iWAT of Wt and *Cyp27a1*$^{-/-}$ mice after Ft1 treatment. Values are mean±SEM (*n*=5–6 per group), $^{*}P<0.05$, $^{**}P<0.01$ *vs.* HFD group by one-way ANOVA with Dunnett's post-test.

Figure 8 Mechanisms of Ft1 on improvement of obesity and insulin resistance. Ft1 activates intestinal *Tgr5* to enhance intestinal GLP-1 release and improves glucose homeostasis. Furthermore, Ft1 increases the hepatic BA production by suppressing intestinal *Fxr–Fgf15* axis. The elevated serum BA levels subsequently activate *Tgr5* in adipose tissues to increase energy expenditure, thereby conferring beneficial metabolic effects in obese mice.

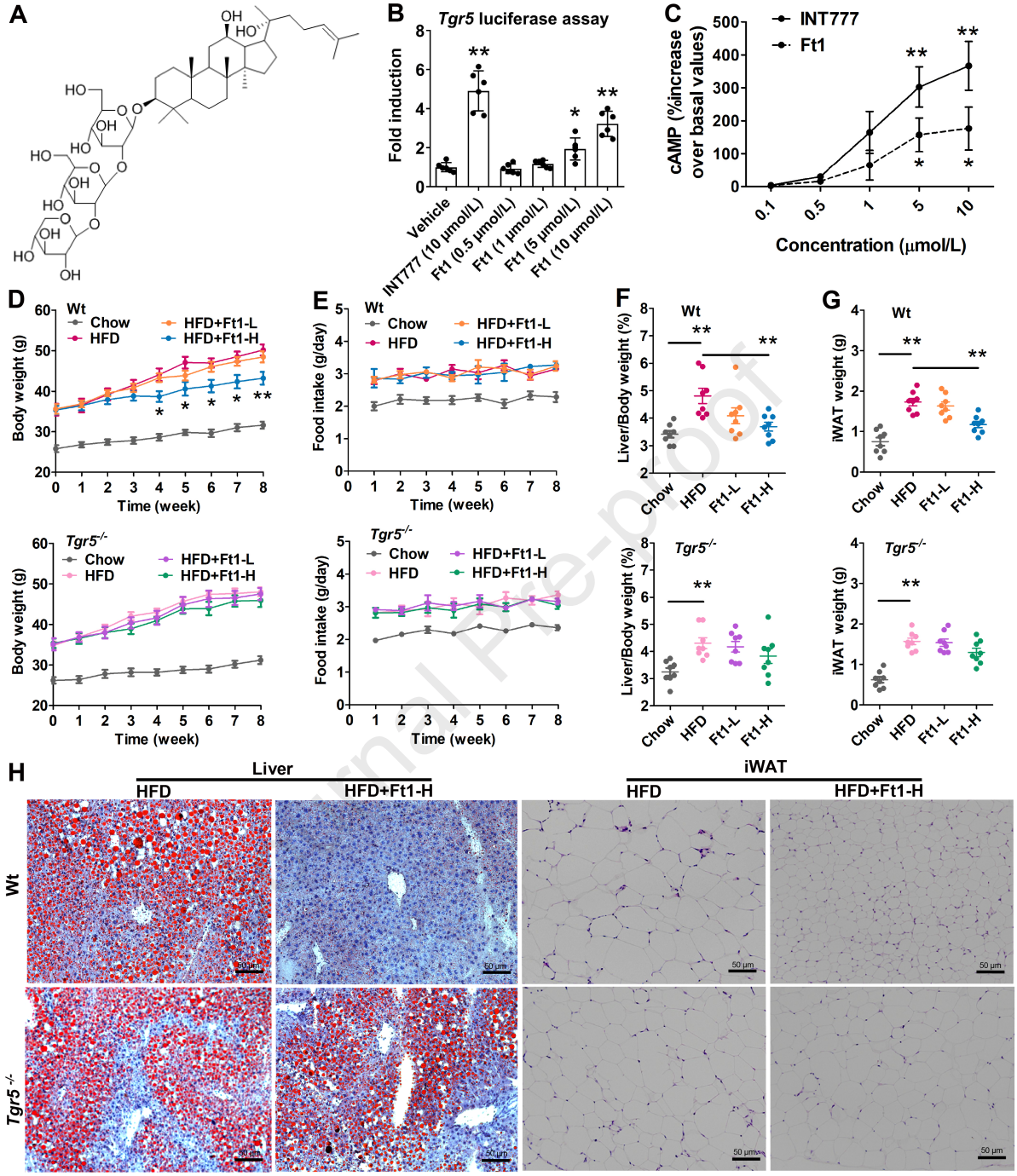
A
B
Tgr5 luciferase assay
Fold induction
Vehicle
INT777 (10 μmol/L)
Ft1 (0.5 μmol/L)
Ft1 (1 μmol/L)
Ft1 (5 μmol/L)
Ft1 (10 μmol/L)
C
INT777
Ft1
cAMP (%increase over basal values)
Concentration (μmol/L)
D
Wt
Chow
HFD
HFD+Ft1-L
HFD+Ft1-H
Body weight (g)
Time (week)
Tgr5-/-
E
Food intake (g/day)
F
Liver/Body weight (%)
G
iWAT weight (g)
Chow
HFD
Ft1-L
Ft1-H
H
Liver
iWAT
HFD
HFD+Ft1-H
Wt
Tgr5-/-
50 μm

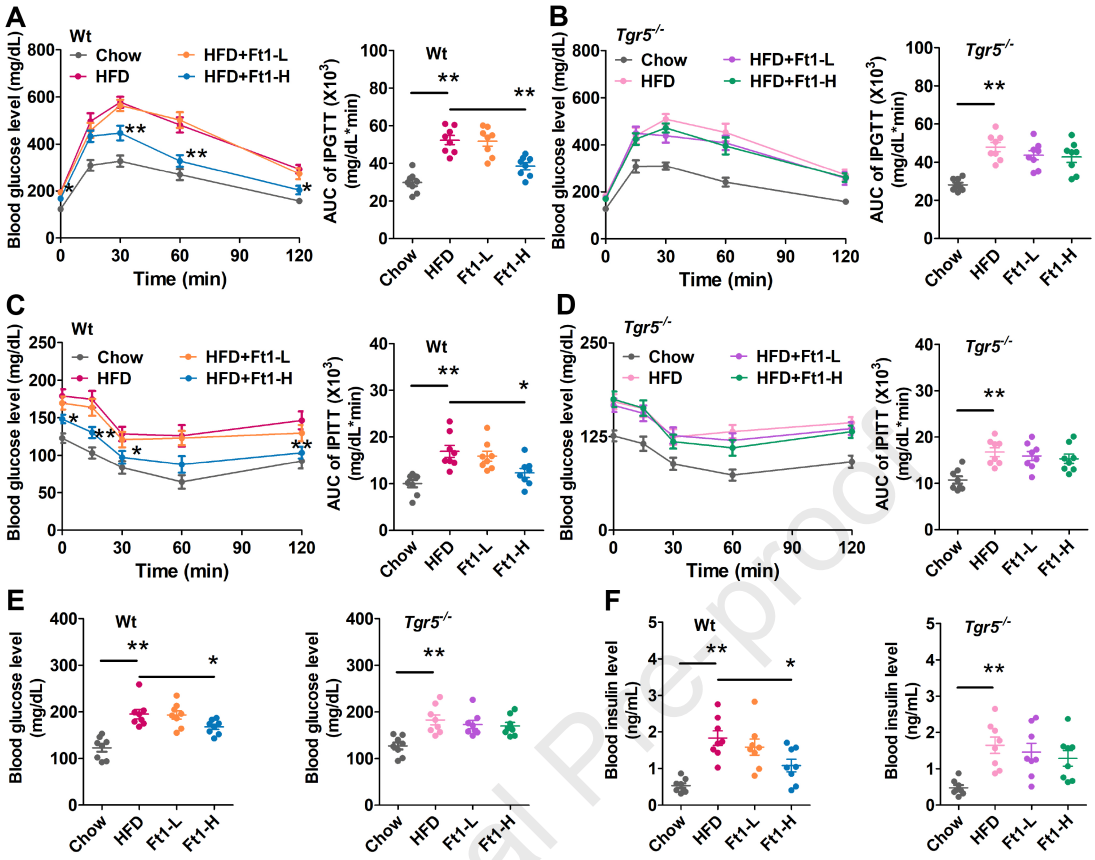

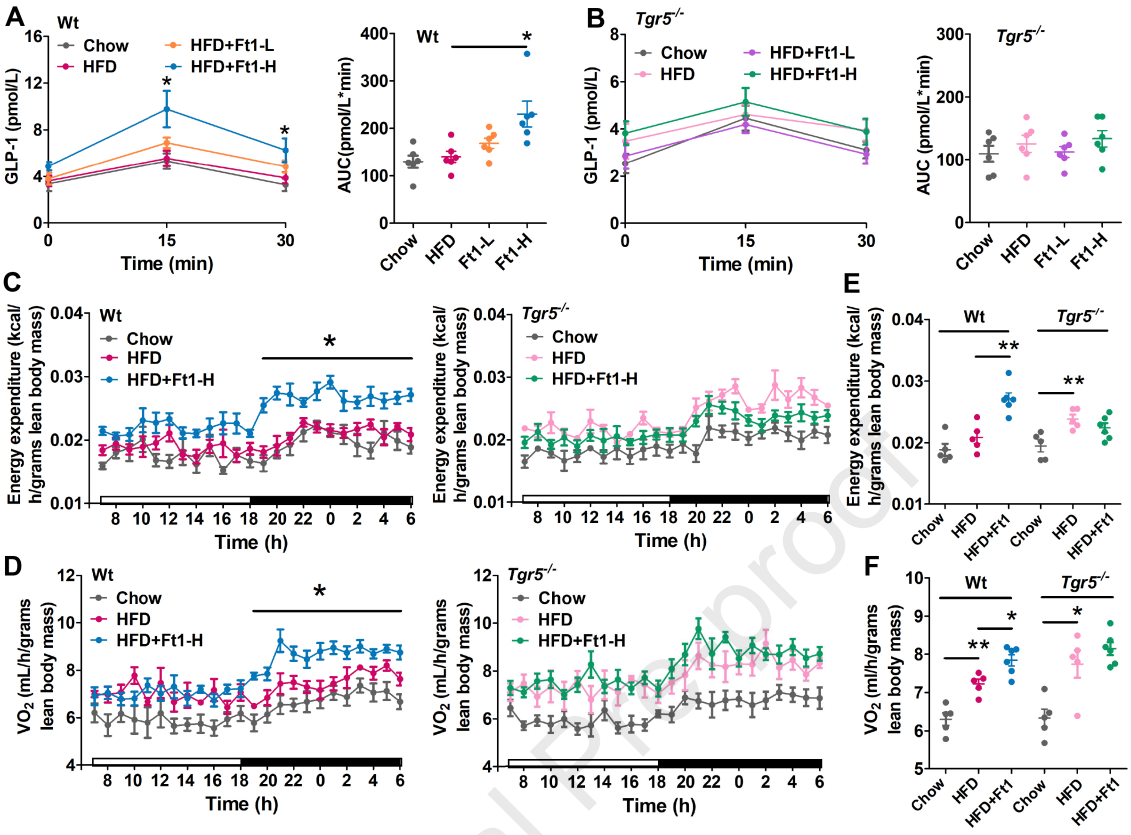

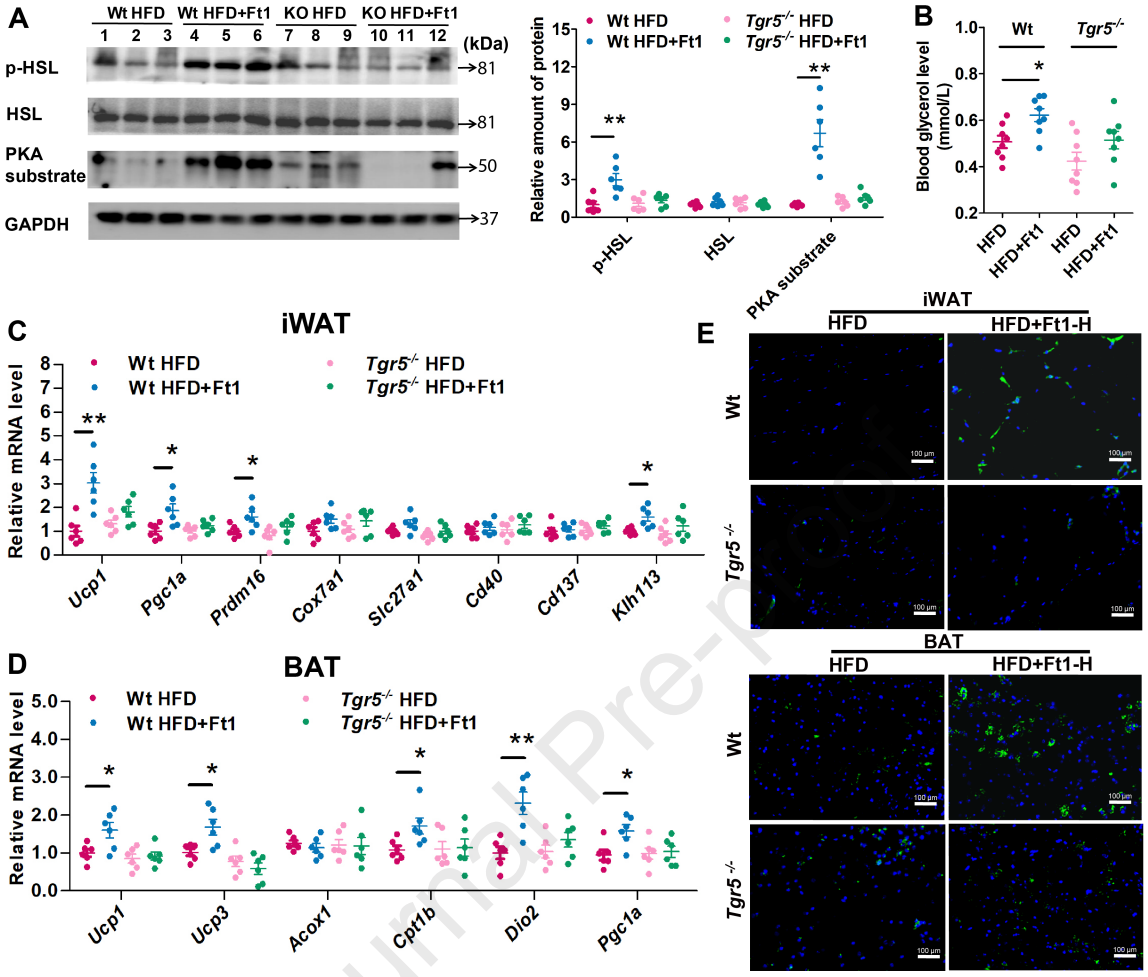
A
Wt HFD
Wt HFD+Ft1
KO HFD
KO HFD+Ft1
1 2 3 4 5 6 7 8 9 10 11 12
(kDa)
p-HSL
HSL
PKA substrate
GAPDH
→81
→81
→50
→37
Relative amount of protein
Wt HFD
Wt HFD+Ft1
Tgr5-/- HFD
Tgr5-/- HFD+Ft1
p-HSL
HSL
PKA substrate
B
Blood glycerol level (mmol/L)
Wt
Tgr5-/-
HFD
HFD+Ft1
C
iWAT
Relative mRNA level
Ucp1
Pgc1a
Prdm16
Cox7a1
Slc27a1
Cd40
Cd137
Klh113
D
BAT
Relative mRNA level
Ucp1
Ucp3
Acox1
Cpt1b
Dio2
Pgc1a
E
iWAT
HFD
HFD+Ft1-H
Wt
Tgr5-/-
BAT
HFD
HFD+Ft1-H
Wt
Tgr5-/-

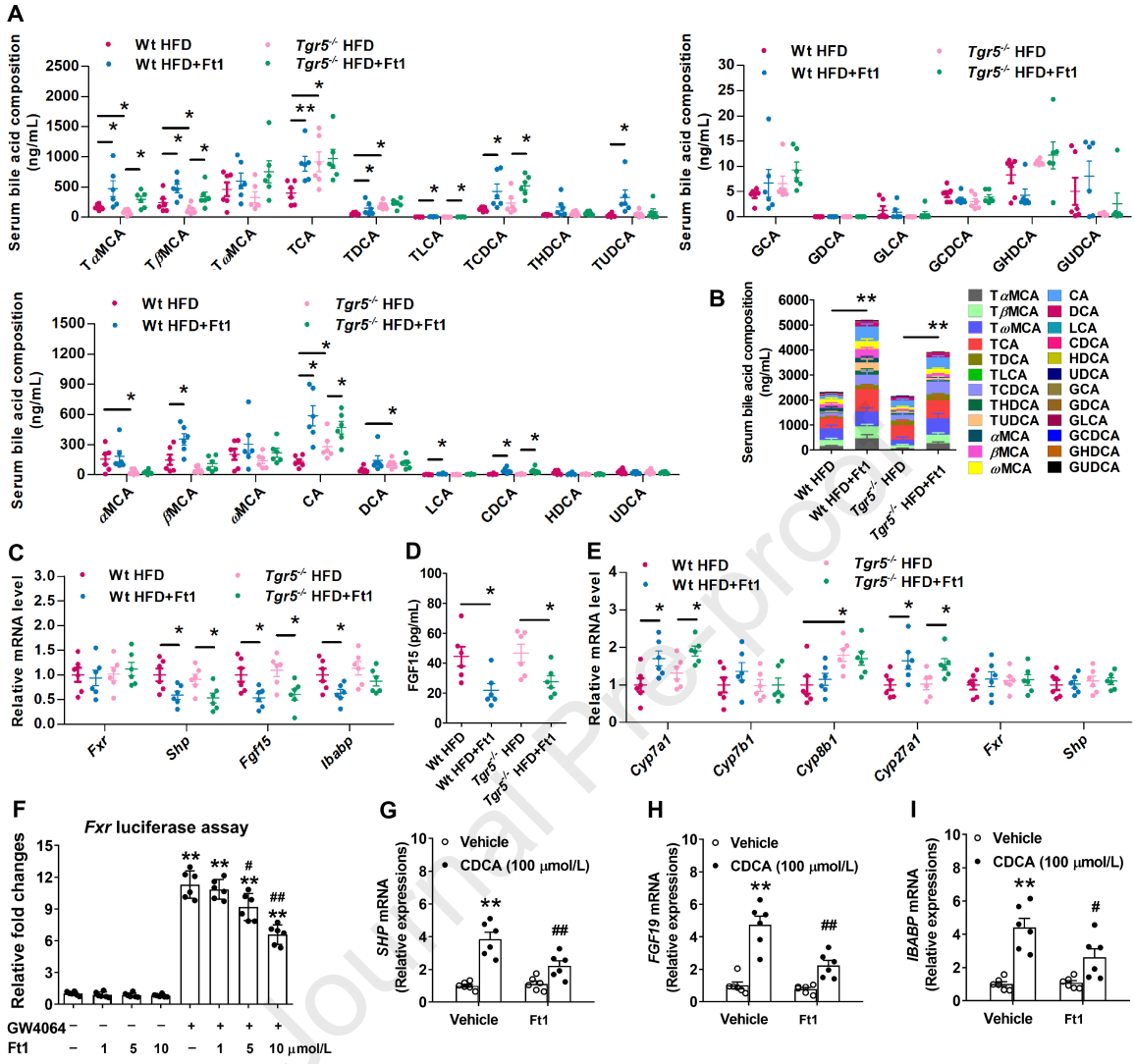
A
Wt HFD
Wt HFD+Ft1
Tgr5-/- HFD
Tgr5-/- HFD+Ft1
Serum bile acid composition (ng/mL)
TαMCA
TβMCA
TωMCA
TCA
TDCA
TLCA
TCDCA
THDCA
TUDCA
GCA
GDCA
GLCA
GCDCA
GHDCA
GUDCA
αMCA
βMCA
ωMCA
CA
DCA
LCA
CDCA
HDCA
UDCA
B
GCA
GDCA
GLCA
GCDCA
GHDCA
GUDCA
C
Relative mRNA level
Fxr
Shp
Fgf15
Ibabp
D
FGF15 (pg/mL)
E
Cyp7a1
Cyp7b1
Cyp8b1
Cyp27a1
F
Fxr luciferase assay
Relative fold changes
GW4064
Ft1
G
SHP mRNA (Relative expressions)
Vehicle
CDCA (100 μmol/L)
H
FGF19 mRNA (Relative expressions)
I
IBABP mRNA (Relative expressions)